Journal of
Marine Science and Technology

Volume 24 | Issue 4 Article 6

NOVEL FAULT DIAGNOSIS METHOD BASED ON CHAOS EYES AND EXTENSION NEURAL NETWORK FOR WIND POWER SYSTEMS

Meng-Hui Wang
Department of Electrical Engineering, National Chin-Yi University of Technology, Taiwan, R.O.C

Pi-Chu Wu
Department of Marketing and Logistics, China University of Technology, Taiwan, R.O.C., jessywu1123@gmail.com

Recommended Citation
Wang, Meng-Hui and Wu, Pi-Chu (2016) "NOVEL FAULT DIAGNOSIS METHOD BASED ON CHAOS EYES AND EXTENSION NEURAL NETWORK FOR WIND POWER SYSTEMS," *Journal of Marine Science and Technology*: Vol. 24: Iss. 4, Article 6.
DOI: 10.6119/JMST-016-0202-1
Available at: https://jmstt.ntou.edu.tw/journal/vol24/iss4/6

Journal of Marine Science and Technology, Vol. 24, No. 4, pp. 717-723 (2016)
DOI: 10.6119/JMST-016-0202-1

NOVEL FAULT DIAGNOSIS METHOD BASED ON CHAOS EYES AND EXTENSION NEURAL NETWORK FOR WIND POWER SYSTEMS

Meng-Hui Wang[1] and Pi-Chu Wu[2]

Key words: wind power system, fault diagnosis, chaos eyes (CEs), extension neural network.

ABSTRACT

This paper proposes a novel approach based on the chaos eye method (CEM) and extension neural network (ENN) for fault diagnosis of wind power systems. First, we used sensors to capture the vibration signals of the wind power system to detect subtle changes. Subsequently, the chaotic synchronization detection method was used to form a chaos error distribution diagram. The distribution diagram centroid, called chaos eye in this paper, was used as the fault diagnosis feature to reduce the number of extracted features. This reduction in diagnostic features enables considerably reducing the computation time and cost of hardware implementation. The ENN-based method was then used to design a fault diagnosis system for the tested wind power generation. The feasibility and practicability of the proposed method were validated using a simulation system. The patent for the proposed method is currently pending, and this method contributes to the key technologies of large-scale wind power generation systems in Taiwan.

I. INTRODUCTION

With rising environmental awareness, the public has begun paying attention to environmental protection; green energy is one of the solutions proposed for reducing environmental pollution (Bull, 2001). Taiwan has limited natural resources and has typically relied on international resource imports. To effectively develop new energy resources, the Taiwan government proposed the Guidelines for Sustainable Energy Policy in 1997, outlining and promoting the National Science Technology Program in Energy. The program was created to facilitate examining and developing carbon-free renewable energy sources, endeavoring to foster renewable energy use and increase the gross power output generated using renewable energy to 8% of total power generation by 2025. The Bureau of Energy, under the Ministry of Economic Affairs, has actively promoted the development of green energy, establishing goals for energy conservation and carbon reduction. The government proposed increasing annual energy efficiency by 2% within the 8 years following 2008 and reducing energy intensity. Regarding CO_2 emissions, the government established goals of reducing carbon emissions to the 2005 level by 2020, and then to the 2000 level by 2025. Taiwan is a small island with a land area of 35,915 km^2. Although its land area is smaller than those of many other countries, Taiwan has relatively abundant wind resources that facilitate developing wind power systems, yielding a wind power output of 132 TWh annually. The offshore island areas, central and southern shore areas, and Hsinchu City in Taiwan are suitable for developing and installing wind power generators. Currently, more than 200 wind power generators exist in Taiwan, yielding an installed capacity exceeding 550 MW (Lu et al., 2000; Liang, 2005).

Renewable energy has advanced in the past decade, with solar photovoltaic power, hydroelectric power, wind power, and fuel cells being prominent research topics. Wind power has been developed and promoted since 1996, and the total installed capacity of global wind power generators has rapidly increased. In 2011, the total installed capacity exceeded 200,000 MW, reaching nearly 250,000 MW. Taiwan has explored wind power since 2002, rapidly expanding the installed capacity of its wind power generator; in 2001, the total installed capacity surpassed 500 MW. Fig. 1 shows the total installed wind power generation capacity in Taiwan during 2002-2012, indicating that Taiwan is a suitable location for developing wind power.

Wind turbines are expensive, and the fault occurrence probability of any power generation system rises after any long-term operation (Lu et al., 2000; Kusiak and Li, 2011). From the data of Swedish wind power plants during 1997-2005, we determined that certain parts of wind power generators breakdown more easily compared with other parts, and that the maintenance time is considerable, which affects the output efficiency of wind power plants (Ribrant and Bertling, 2007).

Paper submitted 01/24/15; revised 11/18/15; accepted 02/02/16. Author for correspondence: Pi-Chu Wu (e-mail: jessywu1123@gmail.com).
[1] *Department of Electrical Engineering, National Chin-Yi University of Technology, Taiwan, R.O.C.*
[2] *Department of Marketing and Logistics, China University of Technology, Taiwan, R.O.C.*

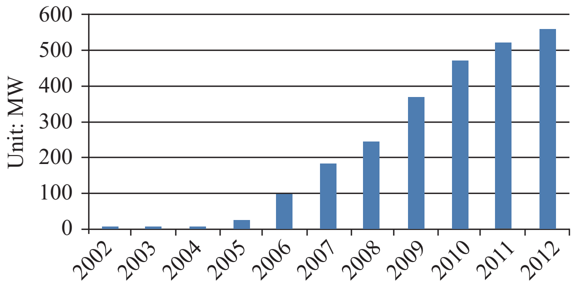

Fig. 1. Total capacity of Taiwan wind power units during 2002-2012.

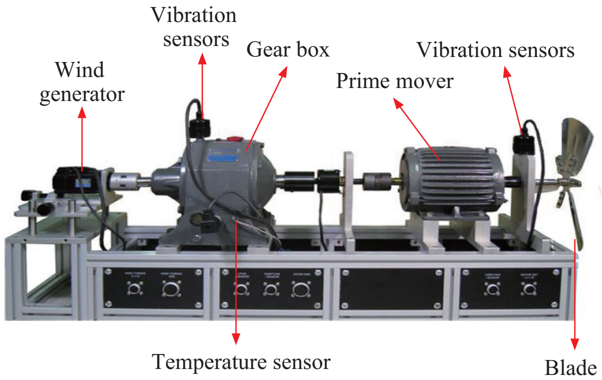

Fig. 2. Experimental platform for the wind power generation system of this study.

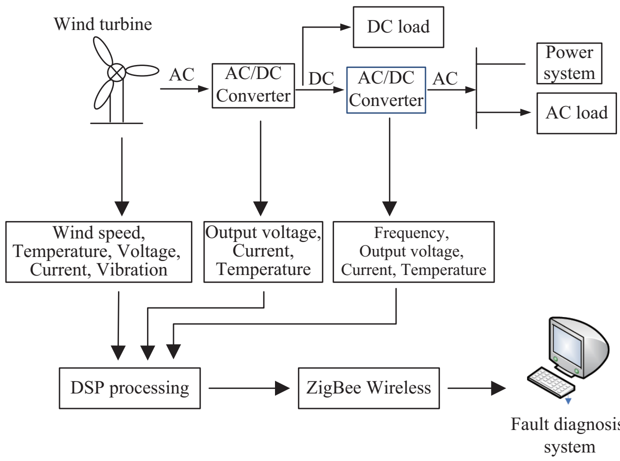

Fig. 3. Fault diagnosis system.

Designing a system that can analyze the extract signals of operational status, forecast the trends and fault state of the operation, and send the results back to the control center through wireless communication networks in real time for maintenance is imperative (Callaway et al., 2002; Lee et al., 2007). Such a system enables adjusting the operating mode, which prevents the wind power generator from accidents. Moreover, we can ensure the safe operation of the system, increase management efficiency, and reduce operation and maintenance costs.

When the attraction to wind electric power generation increases, a higher number of fault detection systems involving more functions, such as trouble shooting external problems, are implemented. Consider, for example, offshore wind power generation systems. Fault detection systems here can eliminate the vibration engendered by the seawater impact (Nilsson and Tjerberg, 2007). The recognition accuracy is obviously high, but the fault system is applicable only when distinguishing the state. When a machine is damaged because of a fault, the lifetime of the wind turbine is shortened. Most fault diagnosis systems for wind power generation increase or reduce the number of sensors according to the accuracy of the system. When the characteristic number is higher, more sensors are required, and the cost is also higher (Caselitz and Giebhardt, 2005; Becker and Posta, 2006). In the current study, a chaotic synchronization-based detector module was used to form the main features of the chaos error distribution diagram. The two centroid points (or chaos eyes, CEs) in the diagram were used as fault detection features. The proposed system achieved a high recognition rate by detecting the critical characteristics of a few machines. The proposed ENN-based fault diagnosis method (EBFDM) not only facilitates executing fast adaptive processes for accessing crucial and new information, but also enables shortening learning times relative to those of previous approaches. Moreover, the proposed EBFDM demonstrated higher accuracy, less memory consumption, and more efficient noise rejection ability in an application.

II. FAULT DIAGNOSIS METHOD

1. Experimental Platform Design

The wind power experimental platform designed by our laboratory was refitted for this study (Figs. 2 and 3). Electric and mechanical signals of the wind turbine were captured by sensors and transmitted through the Ethernet to the signal-processing unit of a remote monitoring computer (Lorenz, 1963; Egan, 2005; Yang, 2010). The signal acquisition unit extracted applicable features, and the signal data were stored in the database. The fault forecasting model was then created using the data. Fig. 4 illustrates the fault diagnosis process, which includes signal processing, feature extraction, and fault diagnosis modules. Visual Basic (VB) was used to develop the fault diagnosis tool for the wind power system in this study.

2. Chaotic Synchronization Detection Method

Meteorologist Norton Lorenz proposed chaos theory in 1963 (Lu, 2001). This theory concerns research on the unsteady behavior of nonlinear dynamic systems. Chaotic synchronization, proposed in 1990, is a theory that entails using a certain type of chaotic signal to control another type of chaotic signal, ultimately synchronizing the two signals (Cai, 1997; Yu et al., 2008). The two synchronous chaotic systems are called a master system and a slave system. When the initial values of the master and slave systems are different, the operating trajectories of these chaotic systems also differ. Therefore, a controller is

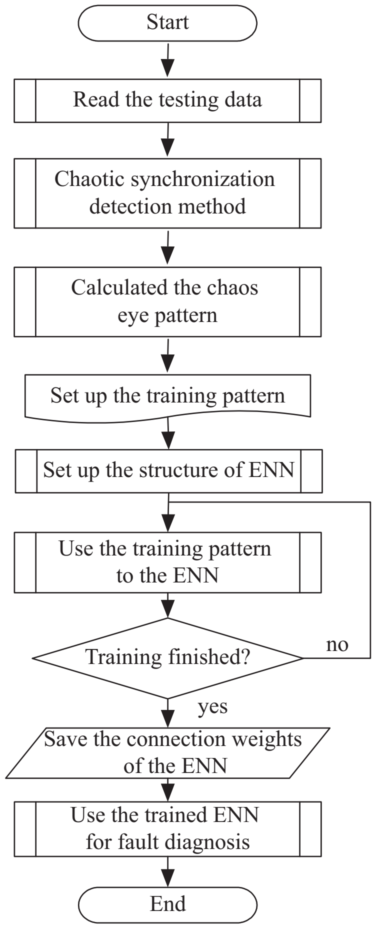

Fig. 4. Overall program flowchart.

attached to the back end of the slave system to track the master system. The controller equalizes the trajectories of the two chaotic systems simultaneously. This tracking state is considered chaotic synchronization, as expressed by Eq. (1).

$$\lim_{t\to\infty} \| X_{Slave,i}(t) - X_{Master,i}(t) \| = 0 \qquad i = 1, 2, \ldots, n \tag{1}$$

In this study, the detection of the chaotic trajectory for system signals was conducted in the simulated system. The master and slave chaotic systems are shown in Eqs. (2) and (3).

$$\text{Master: } \begin{cases} \dot{x}_1 = F_1(x_1, x_2, x_3, \ldots, x_n) \\ \dot{x}_2 = F_2(x_1, x_2, x_3, \ldots, x_n) \\ \vdots \\ \dot{x}_n = F_n(x_1, x_2, x_3, \ldots, x_n) \end{cases} \tag{2}$$

$$\text{Slave: } \begin{cases} \dot{y}_1 = F_1(y_1, y_2, y_3, \ldots, y_n) \\ \dot{y}_2 = F_2(y_1, y_2, y_3, \ldots, y_n) \\ \vdots \\ y_n = F_n(y_1, y_2, y_3, \ldots, y_n) \end{cases} \tag{3}$$

where F_i (i = 1, 2, …, n) is a nonlinear function; Eqs. (2) and (3) form the error state, as shown in Eq. (4). The dynamic error is presented in Eq. (5).

$$e_1 = y_1 - x_1, e_2 = y_2 - x_2, \ldots, e_n = y_n - x_n \tag{4}$$

$$\begin{cases} \dot{e}_1 = F_1(x_1, x_2, x_3, \ldots, x_n) - F_1(y_1, y_2, y_3, \ldots, y_n) = G_1 \\ \dot{e}_2 = F_2(x_1, x_2, x_3, \ldots, x_n) - F_2(y_1, y_2, y_3, \ldots, y_n) = G_2 \\ \vdots \\ \dot{e}_n = F_n(x_1, x_2, x_3, \ldots, x_n) - F_n(y_1, y_2, y_3, \ldots, y_n) = G_n \end{cases} \tag{5}$$

where G_i (i = 1, 2, …, n) is a nonlinear equation, and the dynamic error equation is of a chaotic system. The kinematic trajectory of the attractor of the chaos phenomenon, which is used in the paper, is mostly used to study various system operating states such as the behaviors of periodic, nonperiodic, and random signals. Therefore, the chaotic dynamic error equation was used in this study to recognize the system state. The dynamic error should be multiple data, and the data mode is expressed as follows:

$$\begin{cases} \dot{e}_1[j] = \dot{y}_1[j] - \dot{x}_1[j] \\ \dot{e}_2[j] = \dot{y}_2[j+1] - \dot{x}_2[j+1] \\ \vdots \qquad \vdots \qquad \vdots \\ \dot{e}_n[j] = \dot{y}_n[j+n-1] - \dot{x}_n[j+n-1] \end{cases}, \; j = 1, 2, 3, ..., j-n \tag{6}$$

Two Lorenz chaotic systems were used as examples in this study: a master system and slave system, as expressed in Eqs. (7) and (8), respectively. The dynamic error state equation is established and expressed in matrix form in Eq. (9).

$$\text{Master: } \begin{cases} \dot{x}_1 = \alpha(x_2 - x_1) \\ \dot{x}_2 = \beta x_1 - x_1 x_3 - x_2 \\ \dot{x}_3 = x_1 x_2 - \gamma x_3 \end{cases} \tag{7}$$

$$\text{Slave: } \begin{cases} \dot{y}_1 = \alpha(y_2 - y_1) \\ \dot{y}_2 = \beta y_1 - y_1 y_3 - y_2 \\ \dot{y}_3 = y_1 y_2 - \gamma y_3 \end{cases} \tag{8}$$

$$\begin{bmatrix} \dot{e}_1 \\ \dot{e}_2 \\ \dot{e}_3 \end{bmatrix} = \begin{bmatrix} -\alpha & \alpha & 0 \\ \beta & -1 & 0 \\ 0 & 0 & -\gamma \end{bmatrix} \begin{bmatrix} e_1 \\ e_2 \\ e_3 \end{bmatrix} + \begin{bmatrix} y_2 y_3 - x_2 x_3 \\ -y_1 y_3 + x_1 x_3 \\ y_1 y_2 - x_1 x_2 \end{bmatrix} \tag{9}$$

III. THEORY OF THE EXTENSION NEURAL NETWORK

In certain clustering problems, features are defined as a range of values. For example, the safe operating currents of a specific motor may be between 15 and 20 A. Additionally, *young* can be defined as a cluster of people aged between 18 and 25 years. Appropriately implementing solutions to such problems by using current clustering techniques is difficult. Therefore, a new neural network topology, called extension neural network (ENN), that involves combining extension theory (Wang and Chen, 2012) with neural networks has been proposed for solving these problems (Wang and Hung, 2003; Wang, 2012; Wang and Chen, 2012). In other words, the ENN allows clustering problems to have a range of features, supervised learning, continuous input, and discrete output. This new neural network involves the salient features of parallel computation power and learning capability.

1. ENN Structure

In the fault diagnosis problem of a wind power system, the features and associated defect types cover a range of values. Therefore, the ENN is highly appropriate for resolving the fault diagnosis problem of a wind power system. Fig. 5 illustrates a schematic structure of the ENN, indicating that this structure comprises both an input layer and an output layer. This network involves two connection values (weights) between input nodes and output nodes, with one connection representing the lower bound and the other connection representing the upper bound for this classical domain of features. The connections between the j-th input node and k-th output node are w_{kj}^{L} and w_{kj}^{U}, respectively. The output layer is a competitive layer, meaning that one node exists in the output layer for each prototype pattern; moreover, there exists only one output node with a nonzero output, which indicates the prototype pattern closest to the input vector. The ENN learning algorithm is described as follows.

2. ENN Learning Algorithm

The learning of the ENN can be considered a supervised learning process. Before the learning process, several variables must be defined. Let a training set $\{X_1, T_1\}, \{X_2, T_2\}, \ldots,$ $\{X_Q, T_Q\}$, where Q is the total number of training patterns, represent an input vector to the neural network as well as a corresponding target output. The i-th input vector is $X_i =$ $\{x_{i1}, x_{i2}, \ldots x_{in}\}$, where n is the total number of features. To evaluate the learning performance, the error function is defined as follows:

$$E_t = \frac{1}{2}\sum_{i=1}^{Q}\sum_{j=1}^{n_c}\left(t_{ij} - o_{ij}\right)^2 \tag{10}$$

where w_{ij} represents the desired j-th output for the i-th input pattern and Q_{ij} represents the actual j-th output for the i-th input pattern. The supervised learning algorithm is as follows:

Step 1: Set the connection weights between the input nodes and output nodes according to the range of classical domains. The range of classical domains can be directly derived from previous experience, or it can be determined from training data as follows:

$$w_{kj}^{L} = \min_{T_i \in k}\left\{x_{ij}\right\} \tag{11}$$

$$w_{kj}^{U} = \max_{T_i \in k}\left\{x_{ij}\right\} \tag{12}$$

for $i = 1, 2, \ldots, Q$; $j = 1, 2, \ldots, n$; $k = 1, 2, \ldots, n_c$

Step 2: Read the i-th training pattern and its cluster number p:

$$X_i = \left\{x_{i1}, x_{i2}, \ldots x_{in}\right\} \tag{13}$$

Step 3: Use the extension distance (ED) to calculate the distance between the input pattern X_i and the k-th cluster as follows:

$$ED_{ik} = \sum_{j=1}^{n}\left(\frac{\left|x_{ij} - (w_{kj}^{U} + w_{kj}^{L})/2\right| - (w_{kj}^{U} - w_{kj}^{L})/2}{(w_{kj}^{U} - w_{kj}^{L})/2} + 1\right) \tag{14}$$

for $k = 1, 2, \ldots, n_c$

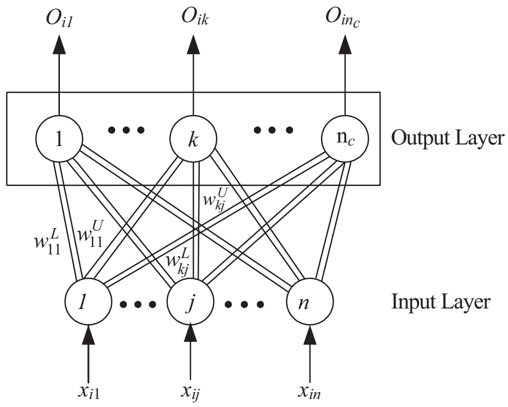

Fig. 5. ENN structure.

The proposed ED is a new distance measure, and it is graphically presented in Fig. 5. The proposed ED can describe the distance between x and a range $\langle w^L, w^U\rangle$, which is different from the traditional Euclidean distance. The dimension of ED is $(i \times N_c)$, and the required memory space for the fault diagnosis system increases when the dimension of ED is considerably high, which also increases the computation time. However, the proposed ENN is a two-layer neural network; therefore, its computation time and memory space are still lower than those of the traditional neural network. Fig. 6 shows that different ranges of classical domains can arrive at different distances because of different sensitivities, and this is a major advantage in classification applications. In general, if

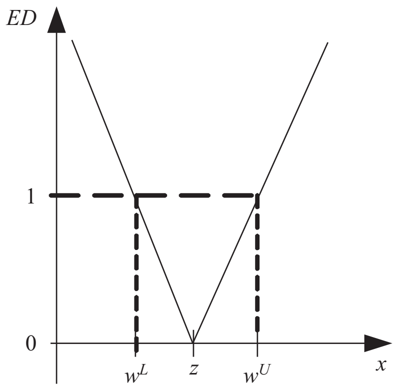

Fig. 6. Proposed ED.

a feature covers a wide range, the data requirement is fuzzy or the sensitivity to distance is low. By contrast, if the feature covers a narrow range, the data precision requirement and sensitivity to distance are high.

Step 4: Find m such that $ED_{im} = \min\{ED_{ik}\}$. If $m = p$, then proceed to Step 6; otherwise, proceed to Step 5.

Step 5: Update the weights of the p-th and m-th clusters as follows:

$$\begin{cases} w_{pj}^{L(new)} = w_{pj}^{L(old)} + \eta(x_{ij} - \dfrac{w_{pj}^{L(old)} + w_{pj}^{U(old)}}{2}) \\ w_{pj}^{U(new)} = w_{pj}^{U(old)} + \eta(x_{ij} - \dfrac{w_{pj}^{L(old)} + w_{pj}^{U(old)}}{2}) \end{cases} \tag{15}$$

$$\begin{cases} w_{mj}^{L(new)} = w_{mj}^{L(old)} - \eta(x_{ij} - \dfrac{w_{mj}^{L(old)} + w_{mj}^{U(old)}}{2}) \\ w_{mj}^{U(new)} = w_{mj}^{U(old)} - \eta(x_{ij} - \dfrac{w_{mj}^{L(old)} + w_{mj}^{U(old)}}{2}) \end{cases} \tag{16}$$

For $j = 1, 2, \ldots, n_c$

where η is a learning rate, which was set to 0.1 in this study. In this step, the learning process involves adjusting only the weights of the p-th and m-th clusters

Step 6: Repeat Steps 2-5, and if all patterns have been classified, then a learning epoch is completed.

Step 7: Stop if the clustering process has converged or the total error has reached a preset value; otherwise, return to Step 3.

The proposed ENN can adopt human expertise before the learning process, and it can produce meaningful output after the learning process because the classified boundaries of the features are clearly determined.

3. Operating Phase of the ENN

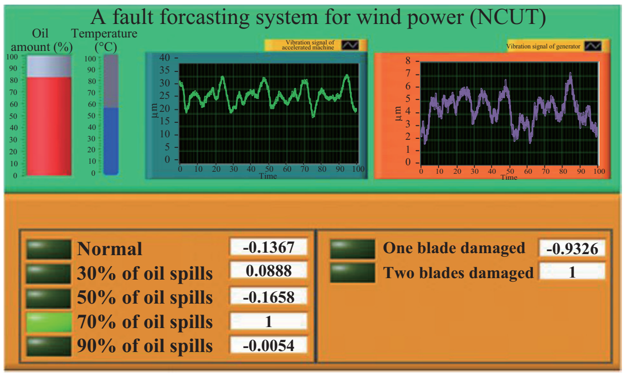

Fig. 7. Man-machine interface I of this study.

Step 1: Read the weight matrix of the ENN.

Step 2: Read a testing pattern

$$X_t = \{x_{t1}, x_{t2}, \ldots, x_{tn}\} \tag{17}$$

Step 3: Use the proposed ED to calculate the distance between the tested pattern and every existing cluster according to Eq. (5).

Step 4: Find m such that $ED_{im} = \min\{ED_{ik}\}$, and set $O_{im} = 1$ to indicate the cluster of the tested pattern.

Step 5: Stop if all the tested patterns have been classified; otherwise, proceed to Step 2.

IV. RESULTS AND DISCUSSION

In this study, VB was used to develop the fault diagnosis tool for the wind power system (Figs. 7 and 8). Ten fault types were diagnosed in the operation of the wind power generation system: normal, fractured blade, crooked blade, 30% of oil spills in the gear accelerator, 50% of oil spills in the gear accelerator, 70% of oil spills in the gear accelerator, 90% of oil spills in the gear accelerator, bearing failure, lack phase, and generator overheat. Sensors were used to capture the values of the generator voltage, gear case vibration, generator vibration, and gear case oil temperature of the wind turbine, and these values were stored in the database. These four primary characteristics were used to form a chaos error distribution diagram by employing a chaotic synchronization-based detector module, and the centroid (or CEs) of the diagram served as the feature. The distribution diagram formed from a primary characteristic had two CEs, and the values of the X and Y axes of the CEs were recorded. Therefore, 16 subcharacteristics were derived; the EBFDM was then used to diagnose the present fault point situation of the wind power system.

We used sensors to capture data under different conditions and stored them in the database. We used 15,000 tested data sets according to the tested wind power system to test the practicability of the proposed method. At the training stage, the training data comprised 10,000 data sets, and the remaining data sets (5000) were used to test the pattern. To detect subtle

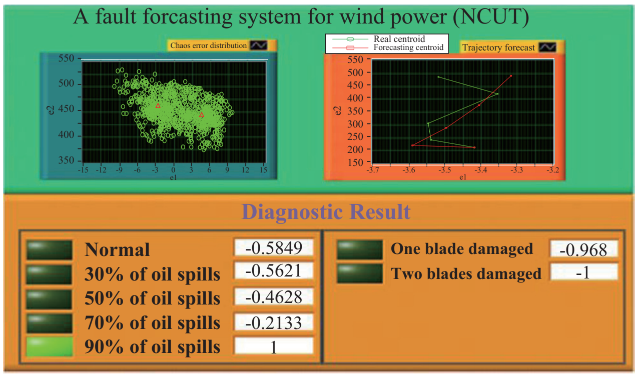

Fig. 8. Man-machine interface II of this study.

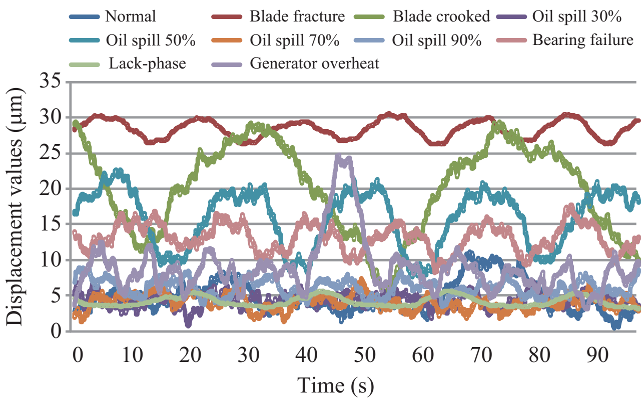

Fig. 9. Gearbox vibration signals.

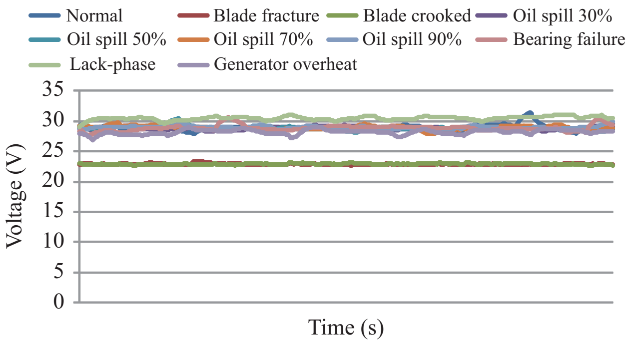

Fig. 10. Generator voltage signal.

changes in the system, we imported the original data into the chaotic synchronization-based detector module to form the chaos error distribution diagram. However, because the diagram contained numerous error distribution points, we used the centroid of the diagram as the characteristic feature for fault diagnosis to effectively set the feature range and reduce the quantity of the extracted features. Fig. 9 illustrates the waveform of the Gearbox Vibration signal, and Fig. 10 presents the waveform of the generator voltage signal. Each time the 1000 documents used for synchronizing the chaos detection module under various fault conditions were read, a different chaotic

Table 1. Accuracy rates of various fault diagnosis methods.

Testing method	Learning times	Learning accuracy rate (%)	Test accuracy rate (%)
Proposed method	2	95.1%	92.9%
K-means clustering method	n/a	80.5%	77.3%
MNN-I	3000	88.2%	85.6%
MNN-II	3000	91.3%	87.3%
MNN-III	3000	89.2%	88.4%

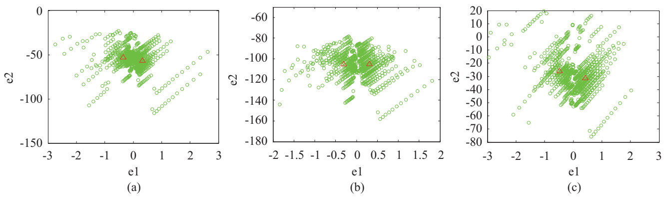

Fig. 11. Chaotic distribution diagram of the generator voltage signals under different conditions, (a) normal state, (b) owe-phase, (c) generator overheat.

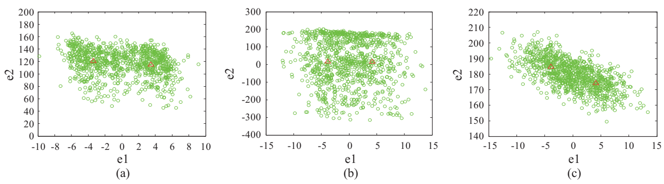

Fig. 12. Chaotic distribution diagram of the bearing vibration signal under different conditions, (a) normal state or no fault, (b) blade crooked, (c) bearing fault.

scatter plot was formed. Fig. 11 shows the chaotic distribution diagram of the generator voltage signals under different conditions: Fig. 11(a) shows a normal state involving no fault, Fig. 11 (b) shows an owe-phase state of output power, and Fig. 11(c) shows the generator overheat condition. The red triangle represents an x-axis positive region and a negative region center of gravity of the chaos error distribution diagram, which is also labeled as CE in Fig. 11. Fig. 12 shows the chaotic distribution diagram of the bearing vibration signal under different conditions: Fig. 12(a) shows a normal state involving no fault, Fig. 12(b) shows the condition involving the crooked blade, and Fig. 12(c) shows the bearing fault.

To evaluate the performance of the proposed EPDRM, the experimental results of the proposed method were directly compared with those of a multilayer neural network (MNN)-based method (Gulski and Krivda, 1992) according to the CE features of the evaluated wind power system (Table 1). Table 1 shows the classification results of the proposed EPDRM for various input patterns. The accuracy rates of the proposed EPDRM were relatively high, and they were approximately 95.1% and 92.9% for the training and testing sets, respectively. Clearly, the ENN has strong generalization capability.

Table 2. Comparison of the classification performance of various methods.

Compare item	Diagnosis methods			
	MNN-I	MNN-II	MNN-III	Proposed ENN
Structure	16-9-10	16-10-10	16-11-10	16-10
No. of connections	1440	1600	1765	320
Learning times (epochs)	3000	3000	3000	2
CPU time (sec)	2350.4	3420.6	4530.2	2.1

Table 2 shows the structures of the various neural network-based diagnosis methods. Notably, the structure of the proposed ENN is highly simple in that it requires only 26 nodes and 320 connections. By contrast, nearly 36 nodes and 1600 connections are required in the structure of the MNN-II-based method. Moreover, the proposed ENN-based method facilitates executing fast adaptive processing for a high amount of training data or new information; this is because the ENN learning process is tuned to only the lower and upper bounds of the excited connections. The ENN also adopts expert experience before the learning process and can produce meaningful output after the learning process; this is because the optimal classified boundaries of the features are clearly determined. Table 2 shows that the proposed ENN exhibits shorter learning time than does the MNN; the ENN also consume sonly 2 epoch or 2.1 s of the CPU time. Although the fault diagnosis system is trained offline, the training time is not a critical point to be evaluated. However, this time is an index that implies, to a certain degree, the efficiency of the algorithm developed, which is rather beneficial when implementing fault diagnosis methods in a microcomputer for a real-time fault diagnosis device or a portable instrument.

V. CONCLUSIONS

This paper presents a novel CE- and ENN-based fault diagnosis method for wind turbine generators. Compared with other existing methods, the structure of the proposed ENN is simpler and its learning time is faster. Moreover, the proposed fault diagnosis method facilitates executing fast adaptive processes for new data because it involves tuning only the boundaries of the classified features or adding a new neural node.

Implementing the proposed method in a microcomputer for portable fault detecting devices is feasible. The conclusions of this study are summarized as follows:

1. This paper proposes that the CE is a new concept for feature determination in the fault diagnosis method for nonlinear energy systems.
2. The chaotic synchronization-based detector module was used to obtain the chaos error distribution from preliminarily captured system signals. The CE was used as a feature, and the fault category was diagnosed according to the CE. The proposed method facilitates reducing the number of extracted features and shortening the program computation time.
3. This novel approach merits more attention because the ENN deserves serious consideration as a tool in PD recognition problems. The findings of this study can lead to further investigation for industrial applications.

REFERENCES

Becker, E. and P. Posta (2006). Keeping the blades turning: Condition monitoring of wind turbine gears. Refocus, 7(2), 26-32.

Bull, S. R. (2001). Renewable Energy Today and Tomorrow. Proceedings of the IEEE 89(8), 1216-1226.

Caselitz, P. and J. Giebhardt (2005). Rotor condition monitoring for improved operational safety of offshore wind energy converters. J. Solar Energy Eng. 127(2), 253-261.

Cai, W. (1997). Extension Engineering Method. Science Press.

Callaway, E., P. Gorday, L. Hester, J. A. Gutierrez, M. Naeve, B. Heile and V. Bahl (2002). Home Networking with IEEE 802.15.4: A Developing Standard for Low-Rate Wireless Personal Area Networks. IEEE on Communications Magazine, 40, 70-77.

Egan, D. (2005). The Emergence of Zigbee in Building Automation and Industrial Controls. IEE Computing & Control Engineering 16(2), 14-19.

Gulski, E. and A. Krivda (1992). Neural networks as a tool for recognition of partial discharges. IEEE Trans. Electrical Insulation 27, 550-556.

Kusiak, A. and W. Li (2011). The prediction and diagnosis of wind turbine faults. Renew. Energy 36(1), 16-23.

Lee, J. S., Y. W. Su and C. C. Shen (2007). A comparative study of wireless protocols: Bluetooth, UWB, ZigBee, and Wi-Fi. The 33rd Annual Conference of the IEEE Industrial Electronics Society (IECON), Taiwan, 46-51, November 5-8.

Liang, C. Y. (2005). The Effects of High Oil Price on the Economy: Discussion on Energy Shortage and the Kyoto Protocol. Almanac of Economic Daily News.

Lorenz, E. N. (1963). Deterministic non periodic flows. J. Atmos. Sci. 20, 130-141.

Lu, M. C. (2001). Piece-wise Synchronization of Lorenz Chaotic Circuit, master's thesis. National Sun Yat-sen University.

Lu, S. M., C. S. Chiu and J. C. Tang (2000). The Global Renewable Energy Development. Energy Quarterly 30(4), 84-93.

Nilsson, J. and L. B. Tjernberg (2007). Maintenance management of wind power systems using condition monitoring systems Life cycle cost analysis for two case studies. IEEE Trans. Energy Conversion 22, 223-229.

Ribrant, J. and Lina Margareta Bertling (2007). Survey of Failures in Wind Power Systems With Focus on Swedish Wind Power Plants During 1997-2005. IEEE Transactions on Energy Conversion 22(1), 167-173.

Wang, M. H. (2012). Application of Extension Neural Network Type-1 to Fault Diagnosis of Electronic Circuit. Mathematical Problems in Engineering. Article ID 352749, 12 pages.

Wang, M. H. and M. J. Chen (2012). Two-Stage Fault Diagnosis Method Based on the Extension Theory for PV Power Systems. International Journal of Photo energy. Article ID 892690, 10 pages.

Wang, M. H. and C. P. Hung (2003). Extension neural network and its applications. Neural Networks 16, 779-784.

Yang, J. C. (2010). Application of Wireless Sensors to Fault Diagnosis for Wind Power Generation System. master's thesis, National Chin Yi University of Technology.

Yu, H., S. C. Chu and S. Y. Liu (2008). Multi-stable Synchronization Manifold in Generalized Synchronization of Chaos, Graduate Institute of Vibration Noise. Naval University of Engineering, Act a Mathematica Scientia 57(5), 35-4.